The Astrophysical Journal, xxx: xxx–xxx, 2008 XXX xx

ON THE DISTRIBUTION OF STELLAR MASSES IN GAMMA-RAY BURST HOST GALAXIES[1]

J. M. Castro Cerón[2], M. J. Michałowski[2], J. Hjorth[2], D. Malesani[2],
J. Gorosabel[3], D. Watson[2], and J. P. U. Fynbo[2]

Received 2008 March 12; accepted 2008 XXX xx; published 2008 XXX xx

ABSTRACT

We analyse *Spitzer* images of 30 long-duration gamma-ray burst (GRB) host galaxies. We estimate their total stellar masses ($M_\star$) based on the rest-frame K-band luminosities and constrain their unobscured star-formation rates (SFR) based on the rest-frame UV continuua. Further, we compute a mean $M_\star/L_{K_{\rm rest}} = 0.45\,M_\odot/L_\odot$. We find that the hosts are low $M_\star$, star-forming systems. The median $M_\star$ in our sample ($\langle M_\star\rangle = 10^{9.7}\,M_\odot$) is lower than that of "field" galaxies (e.g., Gemini Deep Deep Survey). The range spanned by $M_\star$ is $10^7\,M_\odot < M_\star < 10^{11}\,M_\odot$, while the range spanned by the unobscured SFR is $10^{-2}\,M_\odot\,{\rm yr}^{-1} < {\rm SFR} < 10\,M_\odot\,{\rm yr}^{-1}$. There is no evidence for intrinsic evolution in the distribution of $M_\star$ with redshift. We show that extinction by dust must be present in at least 25% of the GRB hosts in our sample, and suggest that this is a way to reconcile our lower, UV-based, specific SFR ($\phi \equiv {\rm SFR}/M_\star$) with previous claims that GRBs have some of the highest ϕ values. We also examine the effect that the inability to resolve the star-forming regions in the hosts has on ϕ.

Subject headings: cosmology: observations — dust, extinction — galaxies: fundamental parameters — galaxies: ISM — gamma rays: bursts — infrared: galaxies

1. INTRODUCTION

It is central to contemporary cosmology to map the build-up of cosmic structure and star-formation (SF); and we know that the detection of a gamma-ray burst (GRB) is an indication that its host galaxy harbors massive SF. GRBs are pulses of γ-rays from sources of cosmological origins, and are the most luminous, photon-emitting events in the universe. As tracers of SF they have fundamental advantages: dust extinction has essentially no effect in their detection at γ-ray and X-ray wavelengths; GRBs can be observed to very high redshifts; these redshifts can be measured from afterglow spectroscopy independently of the host magnitudes; and the selection of GRBs is independent of the host galaxy luminosity at any wavelength. That is to say that GRBs are unique eyes to gainfully look at the star-forming universe. But the following critical questions should be answered in order to use GRBs as tracers of SF: What is the level of bias in optically-selected GRB host samples? And what is the intrinsic bias in the GRB-SF rate?

A canonical model is well established for long-duration GRBs: they occur in star-forming regions in star-forming galaxies (Bloom et al. 2002; Gorosabel et al. 2003a; Christensen et al. 2004; Fruchter et al. 2006) and are associated with stellar core collapse events and hence with high-mass SF (e.g. Galama et al. 1998; Hjorth et al. 2003; Stanek et al. 2003; Zeh et al. 2004; Campana et al. 2006). The emerging picture, however, is complex. Most GRB host galaxies are faint and blue (Fruchter et al. 1999; Le Floc'h et al. 2003). A few hosts show tentative evidence of very high star-formation rates (SFRs; Chary et al. 2002; Berger et al. 2003), but their optical properties do not appear typical of the galaxies found in blind submillimeter galaxy surveys (Tanvir et al. 2004; Fruchter et al. 2006).

It is currently debated how GRB hosts relate to other known populations of star-forming galaxies. At redshifts around 3 the UV luminosities of host galaxies and the metallicities of GRB sightlines are consistent with the expectation if hosts are drawn from the underlying population of all star-forming galaxies weighted with the total SF density per luminosity bin (Jakobsson et al. 2005a; Fynbo et al. 2008). With *Spitzer*'s (Werner et al. 2004) IRAC (Infrared Array Camera; Fazio et al. 2004) mid-infrared (MIR) photometry, together with optical and near-infrared (NIR) data, we can establish how the host galaxies relate to other star-forming populations in terms of total stellar mass ($M_\star$). This is essential if we are to understand the full range of properties of star-forming galaxies at high redshifts and fully exploit the potential of GRBs as probes of cosmic SF.

Castro Cerón et al. (2006) studied a sample of 6 long-duration GRB host galaxies observed with IRAC and MIPS (Multiband Imager Photometer for *Spitzer*; Rieke et al. 2004). They estimated their $M_\star$ based on rest-frame K-band luminosity densities and constrained their SFRs based on the entire available spectral energy distribution (SED). In this work we extend the computations to a sample of 30, but constrain only the unobscured SFRs with the rest-frame UV continuum. This larger sample ought to allow for a more robust statistical analysis, as well as to probe the distribution of $M_\star$ in redshift space. To determine $M_\star$ we utilize rest-frame K flux densities (interpolated from observed IRAC and NIR fluxes). This extends the data set presented by Castro Cerón et al. (2006), yielding accurate values of $M_\star$ in a large host galaxy sample. To determine the unobscured SFRs we use rest-frame UV flux densities

[1] This work is based in part on observations made with the *Spitzer Space Telescope*, which is operated by the Jet Propulsion Laboratory, California Institute of Technology, under a contract with NASA.

[2] Dark Cosmology Centre, Niels Bohr Institute, University of Copenhagen, Juliane Maries Vej 30, DK-2100 Copenhagen Ø, Denmark; josemari@dark-cosmology.dk, michal@dark-cosmology.dk, malesani@dark-cosmology.dk, darach@dark-cosmology.dk, jens@dark-cosmology.dk, jfynbo@dark-cosmology.dk.

[3] Instituto de Astrofísica de Andalucía (CSIC), c/. Camino Bajo de Huétor, 50, E-18.008 Granada, Spain; jgu@iaa.es.

(interpolated from observed optical fluxes). These unobscured SFRs are lower limits to the total SFR of a galaxy due to the possible extinction by dust, and we compare them with those of Castro Cerón et al. (2006). Our paper is organized as follows: An overview of the sample selection is given in §2; The analytic methodology is described in §3. $M_\star$ for the sample are derived in §4, and §5 sees the computation of the unobscured SFRs. We conclude in §6 with analysis and discussion. We assume an $\Omega_m = 0.3$, $\Omega_\Lambda = 0.7$ cosmology with $H_0 = 70\,\mathrm{km\ s^{-1}\ Mpc^{-1}}$.

2. DATA

Our current sample is composed of 30 long-duration GRB host galaxies, three of them within the X-ray flash category (Heise 2003). We made the selection by requiring each host to have rest-frame K-band data available (for the purposes of this work we define $K \equiv 2.2\,\mu\mathrm{m} \pm 0.3\,\mu\mathrm{m}$); thus the $M_\star$ estimator is well calibrated (Glazebrook et al. 2004). An additional requirement for inclusion in the sample was the availability of the redshift.

This 30 GRB host galaxy sample spans a redshift interval $0 < z < 2.7$, with a median value $z \simeq 0.84$. For comparison, the median redshift[4] of those GRBs detected prior to the start of operations of the *Swift* satellite (Gehrels et al. 2004) is $\langle z \rangle \simeq 1.0$, and that of those GRBs detected afterwards is $\langle z \rangle \simeq 2.3$; i.e., in this work we are chiefly looking at the lower end of the GRB redshift distribution. Given the redshifts sampled, the rest-frame K-band data for 24 of the 30 host galaxies were obtained from the *Spitzer* Science Archive, where we examined all publicly available hosts up to (and including) October 2007. The remaining 6 GRB hosts (980425, 030329, 031203, 060218, 060505, and 060614) in the sample have very low redshifts ($z \lesssim 0.1$), so in those cases $K_{\lambda_{\rm obs}} \sim K_{\lambda_{\rm rest}}$ (i.e., $K_{\lambda_{\rm rest}}$ falls within the nominal width of $K_{\lambda_{\rm obs}}$). The sample is presented in Table 1.

Each host (except GRBs 060218, 060505, and 060614) were imaged with IRAC. Detectors are 256×256 squared pixel arrays (scale $= 1\farcs2\,\mathrm{pixel}^{-1} \times 1\farcs2\,\mathrm{pixel}^{-1}$; field of view $= 5.21\,\mathrm{arcmin} \times 5.21\,\mathrm{arcmin}$). The instrumental PSFs (FWHM) are: channel 1 $= 1\farcs66$; channel 2 $= 1\farcs72$; channel 3 $= 1\farcs88$; channel 4 $= 1\farcs98$. The optical and NIR data complementing IRAC in Table 1 were obtained from the literature. Two UV data points (GRBs 980425 and 060505) come from our analysis of *GALEX* (Galaxy Evolution Explorer; Martin et al. 2003, 2005) data.

3. METHODOLOGY

For the MIR photometry we use official *Spitzer* Post Basic Calibrated Data (Post-BCD) products (in Castro Cerón et al. 2006 we carefully verified the Post-BCD with our own reductions). Host extraction is based on the archival imagery world coordinate system calibration and visually confirmed with optical and/or NIR comparison images from the literature. The median separation between the host centroid in each IRAC image and the best set of coordinates published is well below $1''$. GRB 980425 is the only host galaxy resolved in the IRAC images and we have obtained its photometry from the literature (Le Floc'h et al. 2006). None of the other GRB host galaxies of our sample are spatially resolved in the IRAC images, and their flux densities can be estimated using small circular aperture photometry. We measure the flux densities over a circled area of radius 2 pixels. In most cases this allows us to recover the emission of the host while avoiding contamination from other field sources located nearby. But in a few instances there was suspicion that the nearby field sources might be contaminating our host galaxy photometry. As a sanity check we subtracted those field sources and redid the photometry. Field-source subtraction was performed using the detection output image given by the Source Extractor software package (SExtractor; Bertin & Arnouts 1996), where the detected sources were replaced by background noise. The photometry on the field-source-subtracted images was always consistent with the original aperture photometry. Aperture corrections have been applied to account for the extended size of the PSF. Based on the *Spitzer* Science Center recipe for *Estimating Signal-To-Noise Ratio of a Point Source Measurement for IRAC*[5] we calculate conservative errors, including both statistical and systematic estimates. Our flux density measurements and upper limits are given in Table 1, column (3). We find that, of those hosts in our sample observed with channel 1, about 36% are detected. For channel 2 the rate is about 64%. This is roughly of the same order as the detection rate by Le Floc'h et al. (2006) with IRAC channel 2 (44%), though we caution that both samples are incomplete and suffer from selection biases.

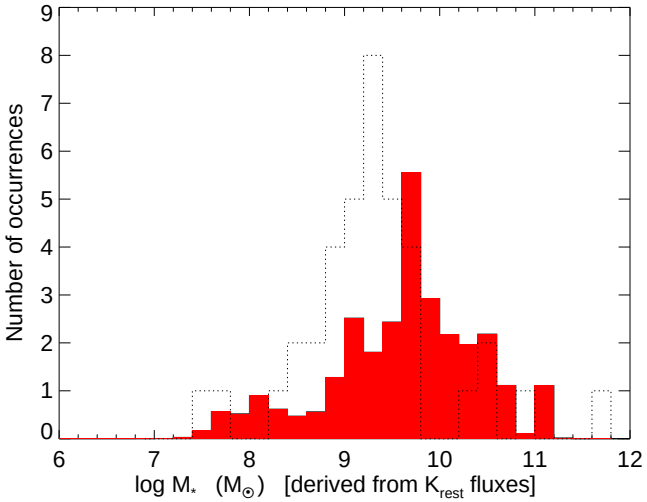

FIG. 1.— Distribution of the total stellar mass ($M_\star$) in GRB host galaxies. *Filled histogram*: 29 out of the 30 hosts in our sample, spanning a redshift interval $0 < z < 1.5$. We note that GRB 030429 has been excluded from the histogram above and the calculation of the median $M_\star$. This is because its host was never detected at any wavelength and, consequently, no lower limit to $M_\star$ can be estimated. The horizontal axis shows the inferred host $M_\star$, derived from interpolated rest-frame K-band flux densities. The median $M_\star$ of the sample is $\langle M_\star \rangle = 10^{9.7}\,M_\odot$. For those host galaxies for which we have upper limits we estimate a conservative lower limit by extrapolating a flat spectrum ($f_\nu \propto \nu^0$) from the reddest NIR/optical detection (references in Table 1, column 4); then we split an area normalized to unit among the bins bracketed by the limits. For each GRB host for which we have detections we assume a normalized Gaussian distribution of the error bars in linear space. Then we allocate $M_\star$ in proportion to the area of the Gaussian in each bin. *Open histogram*: Figure 2 from Savaglio et al. (2007) is shown for comparison.

[4] http://astro.ku.dk/~pallja/GRBsample.html

[5] http://ssc.spitzer.caltech.edu/documents/irac_memo.txt

TABLE 1
HOSTS: FLUX DENSITIES, TOTAL STELLAR MASSES, AND STAR-FORMATION RATES

	Redshift		IRAC		$K_{\rm rest}$ (21 980 Å)			UV$_{\rm rest}$ (2 800 Å)		
GRB Host (1)	z (2)	Ref.	f_ν (μJy) (3)	Ch.	f_ν (μJy) (4)	Refs.	$M_{\star(K)}$ ($10^9\,M_\odot$) (5)	f_ν (μJy) (6)	Refs.	SFR$_{\rm (UV)}$ ($M_\odot\,{\rm yr}^{-1}$) (7)
970228	0.70	1	<3.7	1	<4.2	‡, 30	<5.7	0.34 ± 0.16	48	0.60 ± 0.28
970508	0.83	2	<2.1[a]	2	<1.8	31, 30	<3.5	0.28 ± 0.15	48	0.71 ± 0.38
970828	0.96	3	3.9 ± 0.3[a]	2	3.7 ± 0.3	31, 3	9.5 ± 0.9	<0.44	34	<1.5
980326	∼1.0	4	<2.7	2	<2.6	‡, 30	<7.1	<0.015	49	<0.056
980425	0.0085	5	2 977 ± 101	2	6 389 ± 395	‡[b], 32	1.1 ± 0.1	1 748 ± 173	‡[c], 50	0.39 ± 0.04
980613	1.10	6	38 ± 1[a]	2	42 ± 1	31, 6	142 ± 3	0.83 ± 0.11	6, 30	3.6 ± 0.5
980703	0.97	7	11 ± 1[a]	2	11 ± 1	31, 33	29 ± 2	3.2 ± 0.1	48	10.9 ± 0.3
981226	1.11	8	4.5 ± 0.5[a]	2	4.6 ± 0.5	31, 8	16 ± 2	0.27 ± 0.03	8	1.2 ± 0.1
990506	1.31	9	2.0 ± 0.7	2	2.0 ± 0.8	‡, 34	9.3 ± 3.8	0.20 ± 0.04	34	1.2 ± 0.2
990705	0.84	10	19 ± 1[a]	2	18 ± 1	31, 10	36 ± 2	∼1.8 ± 0.3	10	∼4.7 ± 0.8
000210	0.85	11	3.3 ± 2.0	2	3.2 ± 1.8	‡, 35	6.4 ± 3.6	0.79 ± 0.07	48	2.1 ± 0.2
000418	1.12	9	4.8 ± 1.8	2	5.0 ± 1.9	‡, 36	17 ± 7	1.33 ± 0.04	48	6.1 ± 0.2
000911	1.06	12	<4.3	2	<4.3	‡, 37	<13	0.33 ± 0.08	37	1.4 ± 0.3
010921	0.45	13	11 ± 2	1	12 ± 2	‡, 13	6.5 ± 0.9	2.2 ± 0.1	48	1.6 ± 0.1
020405	0.69	14	<5.4	1	<5.3	‡, 38	<7.0	2.1 ± 0.1	38	3.7 ± 0.2
020813	1.26	15	<2.5	2	<2.6	‡, 38	<11	0.41 ± 0.08	34, 38	2.3 ± 0.5
020819B	0.41	16	97 ± 2	1	104 ± 7	‡, 16	47 ± 3	4.3 ± 2.6	16	2.6 ± 1.5
021211	1.01	17	<2.2	2	<2.2	‡, 38	<6.1	0.20 ± 0.04	38	0.72 ± 0.15
030328	1.52	18	<29	3	<27	‡, 39	<170	0.56 ± 0.08	39	4.6 ± 0.6
030329	0.17	19	<4.9	1	<5.1	‡, 40[d]	<0.37	1.5 ± 0.2	40	0.14 ± 0.02
030429[e]	2.66	20	<7.0	4	<7.3	‡, 20	<124	<0.060	20	<1.3
030528[e]	0.78	21	<4.6	1	<3.8	‡, 41	<6.5	7.2 ± 1.4	41	16 ± 3
031203	0.11	22	216 ± 3[f]	1	192 ± 13[f]	‡, 42	5.3 ± 0.4	119 ± 39[f]	51	4.3 ± 1.4
040924	0.86	23	<2.9	1	<3.2	‡, 38	<6.5	<1.1	38	<2.9
041006	0.72	24	<2.9	1	<3.1	‡, 38	<4.4	<0.98	38	<1.8
050223	0.58	25	18 ± 2	1	18 ± 2	‡, 25	17 ± 1	<8.1	25	<10
050525A	0.61	26	<1.6	1	<1.6	‡, 43	<1.6	<0.48	43	<0.64
060218[e]	0.03	27	···	···	20 ± 6	44	0.052 ± 0.015	15 ± 3	52	0.053 ± 0.010
060505	0.09[g]	28	···	···	298 ± 10	45	5.8 ± 0.2	75 ± 6	‡[c], 45	1.9 ± 0.2
060614	0.13	29	···	···	3.8 ± 0.7	46, 47	0.15 ± 0.03	0.37 ± 0.13	53	0.019 ± 0.006

REFERENCES. — ‡ This work; (1) Bloom et al. 2001; (2) Bloom et al. 1998; (3) Djorgovski et al. 2001; (4) Bloom et al. 1999; (5) Tinney et al. 1998; (6) Djorgovski et al. 2003; (7) Djorgovski et al. 1998; (8) Christensen et al. 2005; (9) Bloom et al. 2003; (10) Le Floc'h et al. 2002; (11) Piro et al. 2002; (12) Price et al. 2002a; (13) Price et al. 2002b; (14) Price et al. 2003; (15) Barth et al. 2003; (16) Jakobsson et al. 2005b; (17) Vreeswijk et al. 2003; (18) Maiorano et al. 2006; (19) Hjorth et al. 2003; (20) Jakobsson et al. 2004; (21) Rau et al. 2005; (22) Prochaska et al. 2004; (23) Wiersema et al. 2004; (24) Soderberg et al. 2006; (25) Pellizza et al. 2006; (26) Foley et al. 2005; (27) Pian et al. 2006; (28) Colless et al. 2001; (29) Della Valle et al. 2006a; (30) Chary et al. 2002; (31) Castro Cerón et al. 2006; (32) Le Floc'h et al. 2006; (33) Vreeswijk et al. 1999; (34) Le Floc'h et al. 2003; (35) Gorosabel et al. 2003a; (36) Gorosabel et al. 2003b; (37) Masetti et al. 2005; (38) Wainwright et al. 2007; (39) Gorosabel et al. 2005a; (40) Gorosabel et al. 2005b; (41) Rau et al. 2004; (42) Malesani et al. 2004; (43) Della Valle et al. 2006b; (44) Kocevski et al. 2007; (45) Thöne et al. 2008; (46) J. Hjorth 2008, priv. comm.; (47) Cobb et al. 2006; (48) Christensen et al. 2004; (49) Bloom et al. 2002; (50) Michałowski et al. 2008, in prep.; (51) Margutti et al. 2007; (52) Sollerman et al. 2006; (53) Mangano et al. 2007.

NOTE. — Because host positions are well determined from previous broadband imaging, upper limits are quoted at the 2σ level, while errors are 1σ. All (UV, optical, NIR, and MIR) flux densities and magnitudes in this table (including those in the table notes) are corrected for foreground Galactic dust-extinction. Corrections to the IRAC wavebands follow Lutz (1999). For the UV, optical and NIR passbands we use the DIRBE/IRAS dust maps (Schlegel et al. 1998). We adopt a Galactic dust-extinction curve A_λ/A_V, parameterized by $R_V \equiv A_V/E(B-V)$, with $R_V = 3.1$ (Cardelli et al. 1989). Col. (3): Our photometry of *Spitzer*'s IRAC, publicly available, archival data (§3). Channel 1 = 3.6 μm; channel 2 = 4.5 μm; channel 3 = 5.8 μm; channel 4 = 8.0 μm. Col. (4): Interpolated flux densities for the rest-frame K-band (§3). The data used were obtained from these references. Col. (5): $M_\star$ derived (§4) from the rest-frame K-band flux densities listed in column (4), with $M_\star/L_{K_{\rm rest}} = 0.4\,M_\odot/L_\odot$. Col. (6): Interpolated flux densities for the rest-frame UV continuum (§3). The data used were obtained from these references. Col. (7): Unobscured SFRs derived (§5) from the rest-frame UV continuum flux densities listed in column (6).

[a] Flux density values are taken from Castro Cerón et al. (2006); we refine their error estimates.

[b] Our photometry of 2MASS XSC Final Release (Two Micron All Sky Survey Extended Source Catalog; released 25 March 2003; Jarrett et al. 2000; `http://www.ipac.caltech.edu/2mass/`), NIR ($K_{\rm S}$-band) archival data for galaxy ESO 184-G082 ($f_{21\,739\,\text{Å}} = 6\,510\,\mu$Jy ± 406 μJy).

[c] Our photometry of *GALEX* (Galaxy Evolution Explorer; Martin et al. 2003, 2005; `http://galex.stsci.edu/`), UV archival data for the host galaxies of GRBs 980425 ($f_{2\,267\,\text{Å}} = 1\,592\,\mu$Jy ± 162 μJy) and 060505 ($f_{2\,267\,\text{Å}} = 72\,\mu$Jy ± 10 μJy).

[d] K-band is the closest passband, blueward of IRAC, for which this host has data available in the literature. It is a poorly constrained upper limit. We make use of it nevertheless, for methodological consistency (see §3). But we note that in this particular case, given the low redshift of the host, a much closer representation of reality is provided by the lower limit $M_\star = 6.4 \times 10^7\,M_\odot$ (extrapolated from J-band and H-band data). This value is fully consistent with those cited by Thöne et al. (2007) and references therein.

[e] X-ray flash.

[f] Because of the low Galactic latitude ($b = -4.6°$) of this host we correct for dust-extinction overestimates. Following the recommendation by Dutra et al. (2003) we scale the Schlegel et al. (1998) reddening value multiplying by 0.75 and adopt $E_{\rm MW}(B-V) = 0.78$ mag. The UV flux density error (column 6) contains the additional 25% uncertainty estimated by Margutti et al. (2007).

[g] Redshift of the 2dFGRS Public Database (Two Degree Field Galaxy Redshift Survey; `http://magnum.anu.edu.au/~TDFgg/`), archival data for galaxy TGS173Z112.

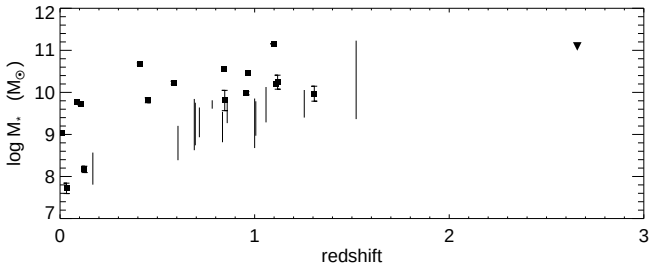

FIG. 2.— Total stellar mass ($M_\star$) as a function of redshift for our 30 GRB host galaxy sample. *Squares*: Detections. *Vertical bars*: Distribution of the non-detection measurements of $M_\star$. The lower limits of these bars were calculated by extrapolating a flat spectrum ($f_\nu \propto \nu^0$) from the NIR/optical data (references in Table 1, column 4).

For each GRB host we compute the flux density at the central wavelength of the rest-frame K-band by means of a linear interpolation in log space. We interpolate between the IRAC channel and the closest passband, blueward of IRAC, for which data are available in the literature. In a few cases the IRAC waveband corresponds to a rest-frame wavelength shorter than K-band, thus we extrapolate. The rest-frame K-band flux densities are shown in Table 1, column (4), along with the appropriate references. In the same fashion we compute, for each host, the rest-frame UV continuum (2 800 Å; Kennicutt 1998) flux density. We either interpolate between the two closest passbands, with data available from the literature, that bracket the rest-frame UV continuum or, when all available data falls redward of 2 800 Å, we extrapolate. These results are shown in Table 1, column (6). In those cases for which only an upper limit to $M_\star$ can be computed we also estimate a conservative lower limit. We do so by extrapolating a flat spectrum ($f_\nu \propto \nu^0$) from the reddest NIR/optical detection available (references in Table 1, column 4). These lower limits are presented as solid bars in Figures 2, 3, and 4.

All flux densities listed in Table 1 are corrected for foreground Galactic dust-extinction (see Table 1 notes for the details). Conversion of the magnitudes obtained from the literature to flux densities is based on Fukugita et al. (1995) for the optical passbands and on Tokunaga & Vacca (2005) and Cohen et al. (2003) for the NIR passbands. The error introduced by the assumption of these photometric systems never dominates over the photometric uncertainties themselves and was safely neglected.

4. TOTAL STELLAR MASSES

We infer $M_\star$ for our sample from rest-frame K-band flux densities. The light emitted by a galaxy in the K-band (e.g., the MIR photometry analyzed in this work) is closely related to its $M_\star$ and thus it is a reliable estimator (Glazebrook et al. 2004). It has little sensitivity to dust since the majority of a galaxy's stellar population has moved away from the birth clouds, and because the NIR bands are virtually unaffected by dust extinction. Such derivation of $M_\star$ is more physically meaningful than an optical/UV luminosity; it effectively integrates over the accumulated $M_\star$ and merger history and can only increase with time, in contrast, for instance, to UV light.

In order to obtain $M_\star$ we apply:

$$M_\star(M_\odot) = 2.67 \times 10^{-48} \times \frac{4\pi D_L^2 f_\nu(\nu_{\rm obs})}{1+z} \times \frac{M_\star}{L_{K_{\rm rest}}}, \quad (1)$$

where for any given object, D_L is its luminosity distance in cm; $f_\nu(\nu_{\rm obs})$ is its flux density at the observed wavelength in μJy; observations should have been made at wavelengths $1.9\,\mu{\rm m} < \nu_{\rm obs}/(1+z) < 2.5\,\mu{\rm m}$ (e.g., this work); and the factor of 2.67×10^{-48} converts the second term in equation 1 to units of solar luminosity. The third term in equation 1, $M_\star/L_{K_{\rm rest}}$, also in solar units, must be estimated for each object.

$M_\star/L_{K_{\rm rest}}$ depends to some extent on the composition of the stellar population (Portinari et al. 2004) or, according to Labbé et al. (2005) who used Bruzual & Charlot (2003) with a Salpeter IMF (Salpeter 1955), on the rest frame $U-V$ colour, age, and $M_\star$. GRB host galaxies are blue, young, and faint (e.g. Le Floc'h et al. 2003; Berger et al. 2003; Christensen et al. 2004). In Castro Cerón et al. (2006) $M_\star/L_{K_{\rm rest}}$ was assumed to be $\sim 0.1\,M_\odot/L_\odot$ to obtain robust lower limits. For this work we compute $M_\star/L_{K_{\rm rest}}$ for GRBs 980703, 000210, and 000418 with the rest-frame K-band flux densities from Table 1, column (4), and $M_\star$ values derived from stellar population model SED fitting (Michałowski et al. 2008), and obtain the following results: $0.29\,M_\odot/L_\odot$ for GRB 980703, $0.63\,M_\odot/L_\odot$ for GRB 000210, and $0.43\,M_\odot/L_\odot$ for GRB 000418. These results yield a mean $M_\star/L_{K_{\rm rest}} = 0.45\,M_\odot/L_\odot$, fully consistent with the average value in Courty et al. (2007), and among the lowest ratios presented by Portinari et al. (2004) for a Salpeter IMF (Salpeter 1955). It is sensible to calculate an average $M_\star/L_{K_{\rm rest}}$ because this ratio is nearly constant, with little dependence on the previous SF history. In fact, $M_\star/L_{K_{\rm rest}}$ varies only by a factor of two between extremely young and extremely old galaxy stellar populations (Glazebrook et al. 2004). So we estimate a conservative $0.4\,M_\odot/L_\odot$ in the calculations of $M_\star$ for our host sample. Table 1, column (5) summarises our $M_\star$ estimates. Errors quoted are statistical. We present a histogram of the distribution of $M_\star$ in log space for our GRB host sample in Figure 1. Van der Wel et al. (2006) examined redshift dependent systematics in determining $M_\star$ from broad band SEDs. They found no significant bias for Bruzual & Charlot (2003) models with a Salpeter IMF (Salpeter 1955).

For comparison we plot Figure 2 from the Savaglio et al. (2007) preliminary analysis in the background of our histogram. The two samples have a 25 object overlap. Our results clearly suggest more massive hosts, about half an order of magnitude higher (median $M_\star = 10^{9.7}\,M_\odot$ in ours vs. median $M_\star = 10^{9.3}\,M_\odot$ in Savaglio et al. 2007; both distributions have a 1σ dispersion of 0.8 dex, and in both cases the average has the same value as the median). Savaglio et al. (2006, 2007) fit the optical-NIR SEDs of their host galaxy sample together with a complex set of SF histories. We can reproduce the median and average $M_\star$ in Savaglio et al. (2007) with our dataset by applying $M_\star/L_{K_{\rm rest}} = 0.2\,M_\odot/L_\odot$ (The Kolmogorov-Smirnov test indicates to a high probability, $p \sim 0.99$ likely because of the 25 object overlap, that our data set and that of Savaglio et al. 2007 come from a population with

the same specific disctribution). Their methodology therefore seems to contain an effective $M_\star/L_{K_{\rm rest}}$ ratio around 0.2. An adjustment by a factor of $\sim$2 to this ratio thus explains the discrepancies in $M_\star$ between our work and that of Savaglio et al. (2007). We note that such an adjustment is within the spread of our calculated values (cf., $0.29\,M_\odot/L_\odot$, $0.43\,M_\odot/L_\odot$, and $0.63\,M_\odot/L_\odot$). The fact that we find larger $M_\star$ may also be indicative of underestimated dust extinction in Savaglio et al. (2007) (see §6).

Our $M_\star$ are always lower than those of the normal $0.4 < z < 2$ galaxies from the Gemini Deep Deep Survey (GDDS; Abraham et al. 2004; Savaglio et al. 2006). The GDDS is a deep optical-NIR ($K < 20.6$) survey complete, for the already mentioned redshift range, down to $M_\star = 10^{10.8}\,M_\odot$ for all galaxies and to $M_\star = 10^{10.1}\,M_\odot$ for star-forming galaxies. In our host sample at least 70% of the galaxies have $M_\star < 10^{10.1}\,M_\odot$. This comparison clearly highlights the efficiency of the GRB selection technique, against that of traditional high-redshift surveys, to pick low-$M_\star$ galaxies at high redshifts.

We plot $M_\star$ as a function of the redshifts for our 30 GRB host galaxy sample in Figure 2 and find no intrinsic correlation between the two variables. The scatter of $M_\star$ is rather uniform across most of the redshift distribution. Hosts with very low $M_\star$ are only found at low redshift. For instance, the four GRB hosts (i.e., 060218, 060614, 030329, and 980425) with the lowest $M_\star$ ($< 10^9\,M_\odot$) have some of the lowest redshift values in our sample. Very low-$M_\star$, high-redshift hosts would have been excluded since most of our largely pre-*Swift* redshifts were measured in emission, what selects preferentially bright host galaxies. Because the redshift is a requirement for inclusion in our sample we are effectively biased against faint systems. This situation has now been corrected in the *Swift* era when most redshifts are secured via afterglow absorption spectroscopy. The upper limits in the vertical bars of Figure 2 (i.e., the distribution for each non-detection measurement of $M_\star$) mark the sensitivity-limited curve for $M_\star$. Conversely, the absence of high-$M_\star$, low-redshift hosts suggests that such GRB host galaxies are rare.

5. STAR-FORMATION RATES

We compute the unobscured SFR for each host by means of their UV continuum luminosity. We convert flux densities into luminosity densities using $L_\nu(\nu_{\rm rest}) = 4\pi D_L^2 f_\nu(\nu_{\rm observed})/(1+z)$ (Hogg et al. 2002). Then we can calculate the unobscured SFRs by applying $\mathrm{SFR}(M_\odot\,\mathrm{yr}^{-1}) = 1.4\times10^{-28} L_{\rm UV}\,(\mathrm{erg\,s^{-1}})$ to the rest-frame $\lambda = 2\,800$ Å flux densities (Kennicutt 1998). The results are summarised in Table 1, column (7). Errors quoted are statistical. In addition there are systematic errors of order 30% (Kennicutt 1998).

The specific SFR $\phi \equiv \mathrm{SFR}/M_\star$ gives an indication of how intensely star-forming a galaxy is. In Figure 3 we plot ϕ versus $M_\star$ for our GRB host sample. The absence of hosts in the lower-left corner is explained as a combination of selection effects and low-number statistics. A host galaxy in this region of the plot has both low $M_\star$ and low SFR, making its detection difficult unless at very low redshifts. As the sampled comoving volume becomes smaller because of the lower redshift required to make a detection, the chance of finding a host decreases accordingly. Given the size of our sample, it is reasonable to expect no detections in this area of the plot. The four GRB host galaxies with the lowest $M_\star$ (GRBs 060218, 060614, 030329, and 980425) are all at very low redshifts and UV bright. We also note that our sample may be biased against low-SFR hosts, since many redshifts have been measured from emission lines. On the other hand, the non-detection of any GRB host in the upper-right corner of Figure 3 should not be due to a selection effect. Such hosts either do not exist or their afterglows were obscured by dust, thus preventing their localization. The sample at hand offers some indication as to the former posibility. Our two host galaxies with the highest $M_\star$ (GRBs 030328 and 980613) would require a dust extinction of $A_V \sim 5$ mag to show there. Yet such dust-extinction levels can be ruled out by the constraints on the SFR from the IR and the radio (see §6 below).

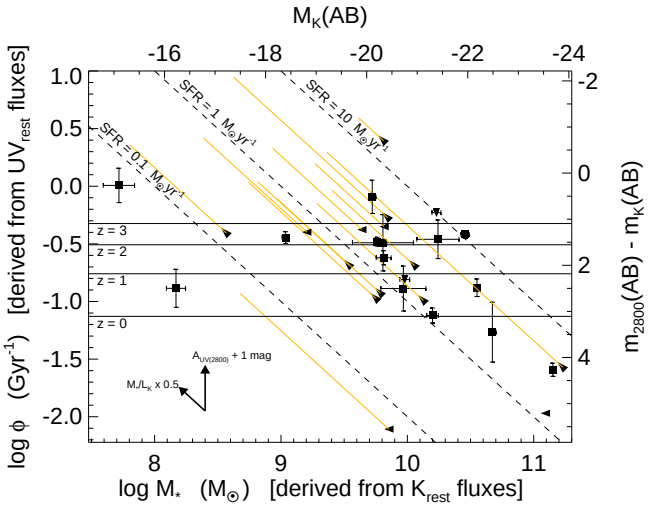

FIG. 3.— Specific SFR (ϕ) as a function of total stellar mass ($M_\star$) for our 30 GRB host galaxy sample. Squares are detections and triangles mark upper limits for either $M_\star$, SFR, or both. *Yellow diagonals*: Equivalent to the vertical bars in Figure 2. Each yellow diagonal could be displaced vertically by the size of the corresponding SFR error bar (Table 1, column 7). *Dashed diagonals*: Constant SFRs of 100, 10, 1, 0.1, and 0.01 $M_\odot\,\mathrm{yr}^{-1}$ respectively. *Black arrows*: Magnitudes of the displacements due to extinction by dust in the UV (e.g., 1 mag; vertical) and changes in our estimation of $M_\star/L_{K_{\rm rest}} \sim 0.4\,M_\odot/L_\odot$ (e.g., a factor of 50%; diagonal). *Right axis*: Color term equivalent to ϕ. *Top axis*: Absolute K-band AB magnitude, equivalent to $M_\star$. The top/right axes represent our GRB host sample in color-magnitude space, effectively equivalent to ϕ vs. $M_\star$.

To exemplify how the estimation of $M_\star/L_{K_{\rm rest}} \sim 0.4\,M_\odot/L_\odot$ affects the location of our hosts in the plot we suppose a 50% uncertainty. We repeat the exercise for an UV-continuum dust-extinction of 1 magnitude. The corresponding displacements are plotted in Figures 3 and 4 with black arrows. The magnitude of these displacements is limited enough not to affect our analysis.

6. ANALYSIS AND DISCUSSION

We find the GRB host galaxies in our current sample possess a wide range of properties; with $10^7\,M_\odot < M_\star < 10^{11}\,M_\odot$; and $10^{-2}\,M_\odot\,\mathrm{yr}^{-1} <$ unobscured SFR $< 10\,M_\odot\,\mathrm{yr}^{-1}$. Yet this diversity points towards low $M_\star$, star-forming systems.

Part of our host sample is extinguished by dust. GRB hosts 970828, 980613, and 990705 (Le Floc'h et al. 2006, 24 μm flux densities; Castro Cerón et al. 2006,

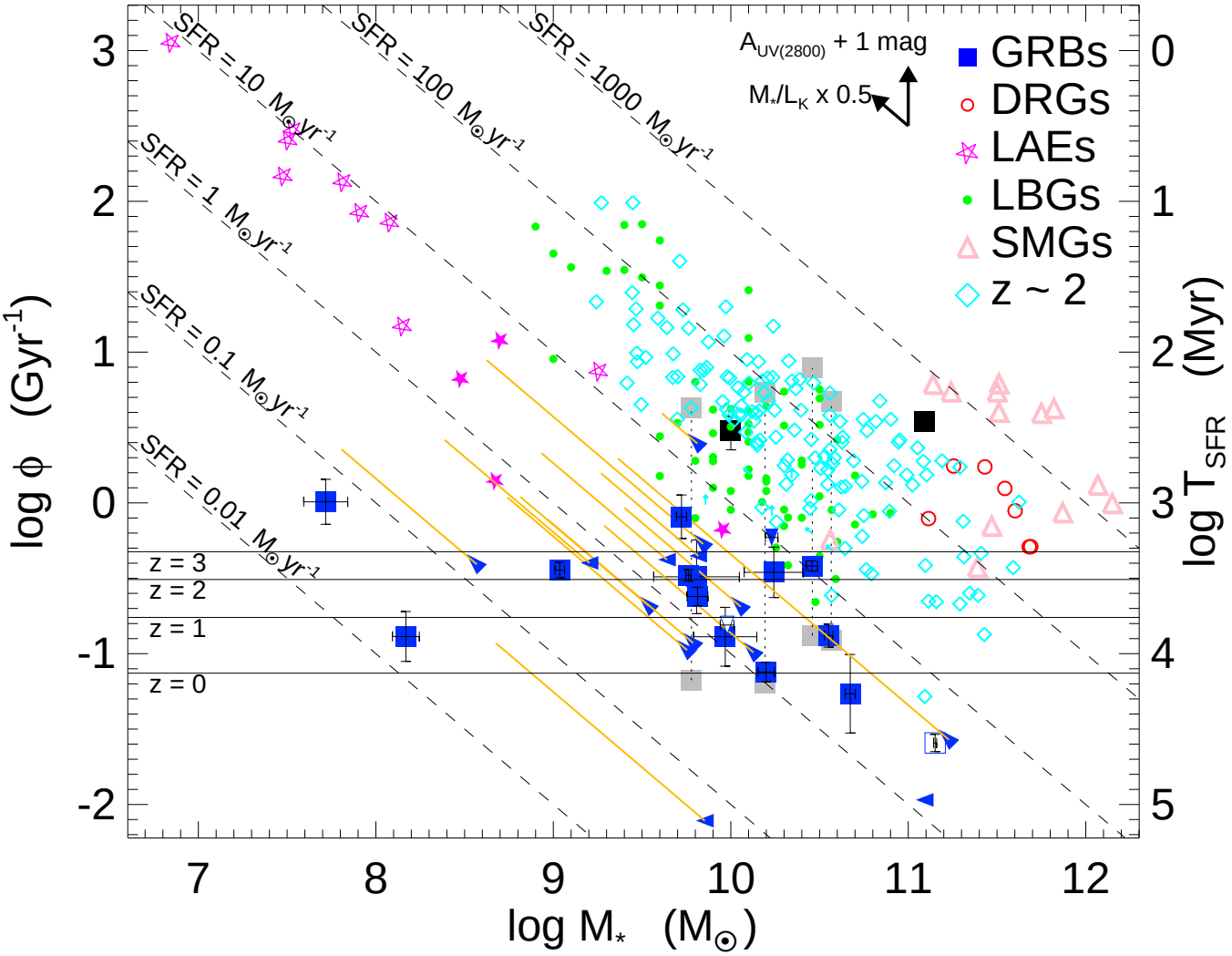

FIG. 4.— Specific SFR (ϕ) as a function of total stellar mass ($M_\star$) for our GRB host galaxy sample and other representative types of galaxies (for a similar plot see Erb et al. 2006; Castro Cerón et al. 2006). *Blue squares and triangles*: Host galaxy sample from this work, with unobscured SFRs derived from the rest-frame UV continuum. Triangles mark upper limits for either $M_\star$, SFR, or both. The open blue triangle and square mark the hosts of GRBs 970828 and 980613 respectively (see §6). *Black squares*: SFR values constrained with a best fit SED model (Castro Cerón et al. 2006). *Grey squares*: Highest/lowest SFR values for those hosts for which a best fit model could not be established (Castro Cerón et al. 2006). Both the black squares and the grey squares have been shifted here correspondingly to compensate for the difference in $M_\star/L_{K_{\rm rest}}$ methodology (i.e., from a lower limit value of $0.1\,M_\odot/L_\odot$ in Castro Cerón et al. 2006 to a best estimated value of $0.4\,M_\odot/L_\odot$ in this work). Yellow diagonals, dashed diagonals, and black arrows are as in Figure 3. *Right axis*: SFR timescale ($T_{\rm SFR} = M_\star/{\rm SFR}$), the inverse of ϕ. On this scale the solid horizontal lines represent the age of the universe for the marked redshift. The distribution of our sample in parameter space suggests that GRBs trace galaxies that are not selected with other techniques. *Data points*: GRBs from this work and Castro Cerón et al. (2006). DRGs from van Dokkum et al. (2004). LAEs from Gawiser et al. (2006), Nilsson et al. (2007), and Lai et al. (2008) (filled stars; average values of the LAE population as a whole, obtained from stacked photometry); N. Pirzkal, S. Malhotra, J. E. Rhoads, & C. Xu (2007, priv. comm.; empty stars; see Pirzkal et al. (2007) for the average values and a description of these sources). Spectroscopically confirmed LBGs from Shapley et al. (2001) and Barmby et al. (2004). SMGs from Borys et al. (2005, $M_\star$) and Chapman et al. (2005, SFR), where we have considered $L_{\rm BOL} \simeq L_{\rm farIR}$, then applied the Kennicutt (1998) calibration. $z \sim 2$ from Erb et al. (2003) and Reddy et al. (2006).

SED fitting), as well as 980703, 000210, and 000418 (Castro Cerón et al. 2006, SED fitting for GRB 980703; Michałowski et al. 2008, SED modelling), have highly obscured SFRs. Additionally several authors argued for dust extinction in the host of GRB 031203 (e.g., Prochaska et al. 2004; Margutti et al. 2007). Applying the recipe in Castro Cerón et al. (2006) to this host galaxy's MIR photometry ($f_{3.6\,\mu{\rm m}} = 216\,\mu{\rm Jy} \pm 3\,\mu{\rm Jy}$; $f_{5.8\,\mu{\rm m}} = 390\,\mu{\rm Jy} \pm 16\,\mu{\rm Jy}$; $f_{24\,\mu{\rm m}} = 13\,103\,\mu{\rm Jy} \pm 41\,\mu{\rm Jy}$; flux densities corrected for foreground Galactic dust-extinction, Lutz 1999; Dutra et al. 2003) we obtain a ${\rm SFR}_{L_{8-1000}} = 13\,M_\odot\,{\rm yr}^{-1}$. That brings the total number of extinguished hosts to at least 7 out of 30, and allows us to crudely estimate that >25% of the sample in this work suffer significant dust extinction ($A_V \gtrsim 1$ mag). Neither our host galaxy sample, nor those others cited in this work, are bias-free. The searches for the GRBs in such samples have been carried out mostly following the localization of an optical afterglow, implicitly biasing the sample against dust-extincted systems. Such potential bias strengthens our statement on dust extinction in GRB host galaxies. Parenthetically, we note that GRBs 970828, 980613, 980703, and 990705 make up two-thirds of a redshift-$z\sim$1-selected, small subsample (Castro Cerón et al. 2006; Le Floc'h et al. 2006). They hint at the possibility that even a higher fraction of hosts

are affected by dust extinction, though with the caveat of low-number statistics.

Castro Cerón et al. (2006) plotted ϕ versus $M_\star$ for six GRB hosts and samples of five other representative types of galaxies: distant red galaxies (DRGs), Lyα emitters (LAEs), Lyman break galaxies (LBGs), submillimeter galaxies (SMGs) and an ensemble of optically-selected, $z \sim 2$ galaxies from the Great Observatories Origins Deep Survey-North field. In Figure 4 we plot, with blue symbols, our 30 host sample using a revised $M_\star/L_{K_{\rm rest}}$ ratio, along with the samples in Castro Cerón et al. (2006). In our ϕ versus $M_\star$ plot (i.e., Figure 4; we use $\mathrm{SFR_{UV}}$) the obscuration of SF by dust pulls the GRB data points down along a vertical line. One way to reconcile the ϕ values of host galaxies in Castro Cerón et al. (2006) and this work is to invoke extinction by dust of the order of $A_V \sim 1$–$3\,$mag (see below). The conversion from $A_{\rm UV}$ to A_V follows Cardelli et al. (1989).

A primary scientific goal in the quantification of galactic evolution is the derivation of the SF histories, as described by the temporal evolution of the star-formation rate, SFR(t). Castro Cerón et al. (2006) noted that their sample had $T_{\rm SFR} < t_{\rm universe}$, allowing for a history of constant SF, with a robust lower limit in $M_\star$ ($M_\star/L_{K_{\rm rest}} \sim 0.1\,M_\odot/L_\odot$). For the sample we present in this work, where we adopt $M_\star/L_{K_{\rm rest}} \sim 0.4\,M_\odot/L_\odot$, clearly few GRB host galaxies are not allowed to have a history of constant SF (i.e., young stars dominating the stellar populations of old galaxies; see the right ordinate axis in Figure 4). Either a starburst episode was present in the past, or a higher recent SFR is required. The latter possibility is consistent with a fraction of GRB hosts having SF obscured by dust. The hosts of GRBs 970828 and 980613 (open blue symbols in Figure 4) are good examples because, under the assumption of constant SF, major dust-extinction must be invoked to account for the age differences. $\phi_{\rm UV}$ estimates result in $T_{\rm SFR} \sim 6\,$Gyr for GRB 970828 and $T_{\rm SFR} \sim 32\,$Gyr for GRB 980613, while ϕ_{L_K} estimates (see Castro Cerón et al. 2006) result in $T_{\rm SFR} \sim 300\,$Myr for both of them. The discrepancies in $T_{\rm SFR}$ imply a dust extinction of the order of $A_V \sim 1.6\,$mag for GRB 970828 and $A_V \sim 2.5\,$mag for GRB 980613. These discrepancies are consistent with the radio-constrained SFR upper limits ($\sim 100\,M_\odot\,\mathrm{yr}^{-1}$ for GRB 970828, and $\sim 500\,M_\odot\,\mathrm{yr}^{-1}$ for GRB 980613) derived by applying the Yun & Carilli (2002) methodology to the deepest radio upper limits reported by Frail et al. (2003).

A dilution effect is present in our MIR photometry. Hosts in our current sample are not spatially resolved in the Spitzer imagery (in the case of GRB 980425 we utilize the total flux of the galaxy for consistency with the rest of the sample). To estimate their $M_\star$ we measure the total K-band light. L_K traces the accumulation of $M_\star$ (Glazebrook et al. 2004) while, most commonly, the SF is ongoing in only a small part of the host galaxy. So we do not normalize our sample's unobscured SFRs by the total stellar mass of the star-forming region(s), rather by $M_\star$, which results in lower ϕ values. This dilution effect pulls the GRB data points in a ϕ versus $M_\star$ plot down along the diagonal (dashed) lines marking constant SFRs.

Extinction by dust, coupled with the dilution effect, could be responsible for the apparent envelope that can be visualized in Figures 3 and 4: a flat plateau with no objects above a certain ϕ value ($\sim 2.5\,\mathrm{Gyr}^{-1}$), and that starts to curve down beyond a particular $M_\star$ ($10^{10}\,M_\odot$). Correcting for dilution and, chiefly, for dust extinction would yield a new plot where our host sample would align consistently with the results/upper limits of Castro Cerón et al. (2006), and provide support to the claim that GRB host galaxies are small and have some of the highest ϕ values.

We conclude by putting forward a simple idea for GRB hosts based on the data analyzed here. As a working hypothesis we suggest that, while low $M_\star$ hosts might contain no dust (i.e., host galaxies with a low $M_\star$ and a low SFR are rare; see §5), progressing upwards in the $M_\star$ distribution of host galaxies will yield significant dust extinction, as well as the already mentioned dilution effect (i.e., the apparent envelope described above for Figures 3 and 4). Our suggestion is consistent with the theoretical predictions presented in Lapi et al. (2008). They further predict that GRB host galaxies trace the faint end of the luminosity function of LBGs and LAEs. Future work (i.e., Herschel observations) on a complete host sample will allow us to test this by quantifying dust extinction and the dilution effect.

The nature of GRBs 060505 and 060614 is strongly debated as no supernova was associated with these long-duration GRBs to deep limits (Fynbo et al. 2006; Gehrels et al. 2006; Della Valle et al. 2006a; Gal-Yam et al. 2006). GRB 060505 falls within the distribution of other long-duration GRB hosts in our sample, whereas GRB 060614 seems to be an outlier. Though this may indirectly suggest that the progenitor of GRB 060614 is different from other typical long-duration GRBs, we note that its SFR is in range with that of the bulk of the sample; and as for $M_\star$, its properties are not very different from some of our other low-redshift host galaxies (e.g., GRBs 060218, 030329, and 980425).

We thank Árdís Elíasdóttir, Peter Laursen, Bo Milvang-Jensen, and Paul M. Vreeswijk for insightful comments. The Dark Cosmology Centre is funded by the Danish National Research Foundation. J. M. C. C. gratefully acknowledges support from the Instrumentcenter for Dansk Astrofysik and the Niels Bohr Instituttet's International PhD School of Excellence. J. G. was funded in part by Spain's AyA 2.004-01.515 and ESP 2.005-07.714-C03-03 grants. The authors acknowledge the data analysis facilities provided by the Starlink Project which is run by CCLRC on behalf of PPARC. This research has made use of: the NASA's Astrophysics Data System; the GHostS database (`http://www.grbhosts.org/`), which is partly funded by Spitzer/NASA grant RSA Agreement No. 1287913; the Gamma-Ray Burst Afterglows site (`http://www.mpe.mpg.de/~jcg/grb.html`), which is maintained by Jochen Greiner; IRAF, distributed by the National Optical Astronomy Observatories, which are operated by the Association of Universities for Research in Astronomy, Inc., under cooperative agreement with the National Science Foundation; the NASA/IPAC Extragalactic Database (NED) which is operated by the Jet Propulsion Laboratory, California Institute of Technology, under contract with the National Aeronautics and Space Administration; and SAOImage DS9, developed by Smithsonian Astrophysical Observatory.

GALEX (*Galaxy Evolution Explorer*) is a NASA Small Explorer, launched in April 2003. We gratefully acknowledge NASA's support for construction, operation, and science analysis for the *GALEX* mission, developed in cooperation with the Centre National d'Etudes Spatiales of France and the Korean Ministry of Science and Technology.

Facilities: Spitzer (IRAC) and *GALEX* (NUV).

REFERENCES

Abraham, R. G., et al. 2004, AJ, 127, 2455
Barmby, P., et al. 2004, ApJS, 154, 97
Barth, A. J., et al. 2003, ApJ, 584, L47
Berger, E., Cowie, L. L., Kulkarni, S. R., Frail, D. A., Aussel, H., & Barger, A. J. 2003, ApJ, 588, 99
Bertin, E., & Arnouts, S. 1996, A&AS, 117, 393
Bloom, J. S., Berger, E., Kulkarni, S. R., Djorgovski, S. G., & Frail, D. A. 2003, AJ, 125, 999
Bloom, J. S., Djorgovski, S. G., & Kulkarni, S. R. 2001, ApJ, 554, 678
Bloom, J. S., Djorgovski, S. G., Kulkarni, S. R., & Frail, D. A. 1998, ApJ, 507, L25
Bloom, J. S., Kulkarni, S. R., & Djorgovski, S. G. 2002, AJ, 123, 1111
Bloom, J. S., et al. 1999, Nature, 401, 453
Borys, C., Smail, I., Chapman, S. C., Blain, A. W., Alexander, D. M., & Ivison, R. J. 2005, ApJ, 635, 853
Bruzual, G., & Charlot, S. 2003, MNRAS, 344, 1000
Campana, S., et al. 2006, Nature, 442, 1008
Cardelli, J. A., Clayton, G. C., & Mathis, J. S. 1989, ApJ, 345, 245
Castro Cerón, J. M., Michałowski, M. J., Hjorth, J., Watson, D., Fynbo, J. P. U., & Gorosabel, J. 2006, ApJ, 653, L85
Chapman, S. C., Blain, A. W., Smail, I., & Ivison, R. J. 2005, ApJ, 622, 772
Chary, R., Becklin, E. E., & Armus, L. 2002, ApJ, 566, 229
Christensen, L., Hjorth, J., & Gorosabel, J. 2004, A&A, 425, 913
———. 2005, ApJ, 631, L29
Cobb, B. E., Bailyn, C. D., van Dokkum, P. G., & Natarajan, P. 2006, ApJ, 651, L85
Cohen, M., Wheaton, Wm. A., & Megeath, S. T. 2003, AJ, 126, 1090
Colless, M., et al. 2001, MNRAS, 328, 1039
Courty, S., Björnsson, G., & Gudmundsson, E. H. 2007, MNRAS, 376, 1375
Della Valle, M., et al. 2006a, Nature, 444, 1050
———. 2006b, ApJ, 642, L103
Djorgovski, S. G., Bloom, J. S., & Kulkarni, S. R. 2003, ApJ, 591, L13
Djorgovski, S. G., Frail, D. A., Kulkarni, S. R., Bloom, J. S., Odewahn, S. C., & Diercks, A. 2001, ApJ, 562, 654
Djorgovski, S. G., Kulkarni, S. R., Bloom, J. S., Goodrich, R., Frail, D. A., Piro, L., & Palazzi, P. 1998, ApJ, 508, L17
Dutra, C. M., Ahumada, A. V., Clariá, J. J., Bica, E., & Barbuy, B. 2003, A&A, 408, 287
Erb, D. K., Shapley, A. E., Steidel, C. C., Pettini, M., Adelberger, K. L., Hunt, M. P., Moorwood, A. F. M., & Cuby, J. G. 2003, ApJ, 591, 101
Erb, D. K., Steidel, C. C., Shapley, A. E., Pettini, M., Reddy, N. A., & Adelberger, K. L. 2006, ApJ, 647, 128
Fazio, G., et al. 2004, ApJS, 154, 10
Foley, R. J., Chen, H.-W., Bloom, J., & Prochaska, J. X. 2005, GCN Circular, 3483
Frail, D. A., Kulkarni, S. R., Berger, E., & Wieringa, M. H. 2003, AJ, 125, 2299
Fruchter, A. S., et al. 1999, ApJ, 519, L13
———. 2006, Nature, 441, 463
Fukugita, M., Shimasaku, K., & Ichikawa, T. 1995, PASP, 107, 945
Fynbo, J. P. U., Prochaska, J. X., Sommer-Larsen, J., Dessauges-Zavadsky, M., & Møller, P. 2008, ApJ, in press (arXiv:0801.3273v1 [astro-ph])
Fynbo, J. P. U., et al. 2006, Nature, 444, 1047
Galama, T. J., et al. 1998, Nature, 395, 670
Gal-Yam, A., et al. 2006, Nature, 444, 1053
Gawiser, E., et al. 2006, ApJ, 642, L13
Gehrels, N., et al. 2004, ApJ, 611, 1005
———. 2006, Nature, 444, 1044
Glazebrook, K., et al. 2004, Nature, 430, 181
Gorosabel, J., Jelínek, M., de Ugarte Postigo, A., Guziy, S., & Castro-Tirado, A. J. 2005a, Il Nuovo Cimento C, 28, 677
Gorosabel, J., et al. 2003a, A&A, 400, 127
———. 2003b, A&A, 409, 123
———. 2005b, A&A, 444, 711
Heise, J. 2003, in AIP Conf. Proc. 662, Gamma-Ray Burst and Afterglow Astronomy 2001, ed. G. R. Ricker, & R. K. Vanderspek (Melville: AIP), 229
Hjorth, J., et al. 2003, Nature, 423, 847
Hogg, D. W., Baldry, I. K., Blanton, M. R., & Eisenstein D. J. 2002, e-print (arXiv:astro-ph/0210394v1)
Jakobsson, P., et al. 2004, A&A, 427, 785
———. 2005a, MNRAS, 362, 245
———. 2005b, ApJ, 629, 45
Jarrett, T. H., Chester, T., Cutri, R., Schneider, S., Skrutskie, M., & Huchra, J. P. 2000, AJ, 119, 2498
Kennicutt, Jr., R. C. 1998, ARA&A, 36, 189
Kocevski, D., et al. 2007, ApJ, 663, 1180
Labbé, I., et al. 2005, ApJ, 624, L81
Lai, K., et al. 2008, ApJ, 674, 70
Lapi, A., Kawakatu, N., Bosnjak, Z., Celotti, A., Bressan, A., Granato, G. L., & Danese, L. 2008, MNRAS, 386, 608
Le Floc'h, E., Charmandaris, V., Forrest, W. J., Mirabel, I. F., Armus, L., & Devost, D. 2006, ApJ, 642, 636
Le Floc'h, E., et al. 2002, ApJ, 581, L81
———. 2003, A&A, 400, 499
Lutz, D. 1999, in ESA SP-427, The Universe as Seen by ISO, ed. P. Cox & M. F. Kessler (Noordwijk: ESA), 623
Maiorano, E., et al. 2006, A&A, 455, 423
Malesani, D., et al. 2004, ApJ, 609, L5
Mangano, V., et al. 2007, A&A, 470, 105
Margutti, R., et al. 2007, A&A, 474, 815
Martin, D. C., et al. 2003, in Proc. SPIE 4854, Future EUV/UV and Visible Space Astrophysics Missions and Instrumentation, ed. J. C. Blades, &, O. H. W. Siegmund (Bellingham: SPIE), 336
———. 2005, ApJ, 619, L1
Masetti, N., et al. 2005, A&A, 438, 841
Michałowski, M. J., Hjorth, J., Castro Cerón, J. M., & Watson, D. 2008, ApJ, 672, 817
Nilsson, K. K., et al. 2007, A&A, 471, 71
Pellizza, L. J., et al. 2006, A&A, 459, L5
Pian, E., et al. 2006, Nature, 442, 1011
Piro, L., et al. 2002, ApJ, 577, 680
Pirzkal, N., Malhotra, S., Rhoads, J. E., & Xu, C. 2007, ApJ, 667, 49
Price, P. A., et al. 2002a, ApJ, 573, 85
———. 2002b, ApJ, 571, L121
———. 2003, ApJ, 589, 838
Prochaska, J. X., et al. 2004, ApJ, 611, 200
Portinari, L., Sommer-Larsen, J., & Tantalo, R. 2004, MNRAS, 347, 691
Rau, A., Salvato, M., & Greiner, J. 2005, A&A, 444, 425
Rau, A., et al. 2004, A&A, 427, 815
Reddy, N. A., Steidel, C. C., Fadda, D., Yan, L., Pettini, M., Shapley, A. E., Erb, D. K., & Adelberger, K. L. 2006, ApJ, 644, 792
Rieke, G., et al. 2004, ApJS, 154, 25
Salpeter, E. E. 1955, ApJ, 121, 161
Savaglio, S., Budavári, T., Glazebrook, K., Le Borgne, D., Le Floc'h, E., Chen, H.-W., Greiner, J., & Yoldaş, A. K. 2007, The Messenger, 128, 47
Savaglio, S., Glazebrook, K., & Le Borgne, D. 2006, in AIP Conf. Proc. 836, Gamma-Ray Bursts in the Swift Era, ed. S. S. Holt, N. Gehrels, & J. A. Nousek (Melville: AIP), 540
Schlegel, D. J., Finkbeiner, D. P., & Davis, M. 1998, ApJ, 500, 525
Shapley, A. E., Steidel, C. C., Adelberger, K. L., Dickinson, M., Giavalisco, M., & Pettini, M. 2001, ApJ, 562, 95
Soderberg, A. M., et al. 2006, ApJ, 636, 391
Sollerman, J., et al. 2006, A&A, 454, 503
Stanek, K. Z., et al. 2003, ApJ, 591, L17
Tanvir, N. R., et al. 2004, MNRAS, 352, 1073
Thöne, C. C., Greiner, J., Savaglio, S., & Jehin, E. 2007, ApJ, 671, 628
Thöne, C. C., et al. 2008, ApJ, 676, 1151
Tinney, C., et al. 1998, IAU Circ., 6896
Tokunaga, A. T., & Vacca, W. D. 2005, PASP, 117, 421
van der Wel, A., Franx, M., Wuyts, S., van Dokkum, P. G., Huang, J., Rix, H. W., & Illingworth, G. D. 2006, ApJ, 652, 97
van Dokkum, P. G., et al. 2004, ApJ, 611, 703
Vreeswijk, P. M., Møller, P., & Fynbo, J. P. U. 2003, A&A, 447, 145
Vreeswijk, P. M., et al. 1999, ApJ, 523, 171
Wainwright, C., Berger, E., & Penprase, B. E. 2007, ApJ, 657, 367
Werner, M., et al. 2004, ApJS, 154, 1
Wiersema, K., Starling, R. L. C., Rol, E., Vreeswijk, P., & Wijers, R. A. M. J. 2004, GCN Circular, 2800
Yun, M. S., & Carilli, C. L. 2002, ApJ, 568, 88
Zeh, A., Klose, S., & Hartmann, D. H. 2004, ApJ, 609, 952